METROLOGICAL ASPECTS OF ABRASIVE TOOL ACTIVE SURFACE TOPOGRAPHY EVALUATION

Dariusz Lipiński, Wojciech Kacalak

Koszalin University of Technology, Faculty of Mechanical Engineering, Racławicka 15-17, 75-620 Koszalin, Poland
(✉ dariusz.lipinski@tu.koszalin.pl, +48 94 3478 295, wojciech.kacalak@tu.koszalin.pl)

Abstract

Analysis of the shape and location of abrasive grain tips as well as their changes during the grinding process, is the basis for forecasting the machining process results. This paper presents a methodology of using the watershed segmentation in identifying abrasive grains on the abrasive tool active surface. Some abrasive grain tips were selected to minimize the errors of detecting many tips on a single abrasive grain. The abrasive grains, singled out as a result of the watershed segmentation, were then analyzed to determine their geometric parameters. Moreover, the statistical parameters describing their locations on the abrasive tool active surface and the parameters characterizing intergranular spaces were determined.

Keywords: grinding wheel, grain segmentation, watershed segmentation, image analysis.

1. Introduction

Abrasive tools used in the grinding process are characterized by an active surface, where a large number of irregularly shaped abrasive grains exist. In typical abrasive machining processes, plunging of a single abrasive grain in the machined material is usually a few to a dozen or so percent of the nominal grain size. These features, as well as the kinematic parameters and machining conditions, determine the effectiveness and energy consumption of the process [1–2].

The parameters describing the shapes and locations of abrasive grains undergo significant changes during the grinding process [3–5]. Changes in the grinding wheel active surface are a result of abrasive wear of the abrasive grain tips, grit fracture and bond fracture, as well as clogging of the grinding wheel active surface. These phenomena lead to losing the cutting ability of abrasive grains or changing their shape. These changes influence the machined surface quality as well as the dimensional accuracy and shape of a workpiece [3–6].

Analysis of the geometric parameters of abrasive grains and the values characterizing their location, as well as analysis of their changes that occur during the grinding process, forms the basis for analysis of the phenomena that occur during the machining process. This analysis is also the basis for the process monitoring systems and makes it possible to evaluate their effectiveness. These phenomena are particularly important in reference to grinding new, often hard-to-cut materials used in the aviation and biomedical industries. The widening scope of applications of these materials requires designing and creating new tools with precisely determined and controlled distributions that describe the shape and location of abrasive grains.

The important elements of research are the systems for modeling and simulating the grinding process. Because of the stochastic nature of the abrasive grain shapes and the random distribution of the tips' geometric parameters, modeling the process becomes a challenging

task. Many research centers have attempted to model the grinding process [3–4, 7–15]. However, many computer simulations of the grinding process were performed using simplified abrasive tool active surface models [11–15]. Such simplified models make analysis and evaluation of the grinding process results more difficult, as they are most often implemented on the level of visual evaluation or general and global parameters.

The current research on the abrasive tool active surface is focused on the influence of its parameters on shaping the topography [16, 17], as well as on evaluation of the cutting ability of abrasive tools, based on analysis of the surface geometric parameters [18]. The detailed analysis of the abrasive tool active surface geometric features requires application of effective methods of detecting abrasive grains. Currently, this analysis is performed using the cut-off plane [19–21]. An advantage of this method is fast detection of the part of active surface of the grinding tool that is in contact with the processed material. However, the increase of the cut-off surface distance from the highest ordinate of the grinding tool causes ambiguity of abrasive grain detection, *e.g.* abrasive grain sets are detected in the place of single grains. The methods of separating abrasive grains used in such cases include only the reciprocal positions of potential tips of abrasive grains.

In this work a methodology of detecting abrasive grains using the watershed segmentation method is proposed. The watershed segmentation is used *e.g.* for motif separation in the surface topography analysis [22, 23]. The main problem of correct abrasive grain detection using this method is preventing the analysed surface from excessive segmentation. Excessive segmentation of abrasive grains results from a large number of local minima on the active surface of a grinding tool.

In the presented research there were performed a series of morphological operations in order to detect tips of abrasive grains. Then, the tips were selected regarding characteristic features of the grinding tool. As a result of the applied method, the abrasive grain borders were obtained, with the surface shaping around the abrasive grain considered. The proposed methodology has been implemented in the MATLAB® environment. Isolating the abrasive grain borders enabled to determine the surface fragments which were then used to determine the abrasive tool active surface topography. The parameters describing the abrasive grains' shape and their location on the abrasive tool active surface were determined, along with the parameters that characterize the volume of intergranular spaces around the abrasive grains.

2. Measuring abrasive tool active surface

Both contact and non-contact techniques are used in the direct abrasive tool surface topography measurements. The abrasive tool active surface measurement can be performed using contact profile-meters [24]. Currently, to measure the grinding wheel active surface, non-contact methods are widely used, including: scanning electron microscopy [8], optical microscopy [9], interference microscopy [10], and laser scanning microscopy [25]. Scanning microscopes that enable to measure the abrasive tool surface directly on the work-station deserve a special attention in this field.

An abrasive tool used in reciprocal internal cylindrical grinding operations with specification 1-35x20x10-SG/F46 M7 VTO was analyzed. The tool contained abrasive grains of microcrystalline sintered alumina SG^{TM} of #46 (356 μm) size, bound with glass-crystalline. The abrasive tool active surface was shaped with a single-grain diamond dresser with a peripheral speed $v_d = 6$ m/s, a depth of dressing $a_d = 0.05$ mm, and an axial table feed speed during dressing cut $v_{fd} = 0.025$ mm/rotation.

A confocal microscope (Olympus® LEXT OLS 4000) with the possibility of performing surface measurements was used to measure the abrasive tool surface. The microscope used for measurement of the grinding tool was equipped with a dual confocal system. This system

enables to measure a tool surface consisting of materials with different light reflection coefficients (abrasive grain material and bond material). The microscope uses a beam of light from the visible spectrum with a wavelength $\lambda = 405$ nm, generated by a class II laser diode.

The obtained spatial representation of the grinding tool active surface is linked to a precise scanning in *x-y* axes. The scanning process is performed by mirror galvanometer scanners deflecting the light beam, so that it hits subsequent points of the surface. The measuring head is located in a motorized vertical travel column, enabling to precisely move along a distance of 70 mm. The subsequent image cross-sections are acquired and then processed in order to obtain a spatial representation of the studied object or its data in the form of a point cloud.

Five specimens of the abrasive tool surface sized 1280 μm × 1280 μm were measured. As a result, a digital abrasive tool surface model was obtained, in which the image pixel value corresponds to the abrasive tool active surface ordinate:

$$z = \mathrm{f}(x, y) | (x, y, z) \in \mathbb{Z}^3. \tag{1}$$

An example of the abrasive tool active surface is presented in Fig. 1a.
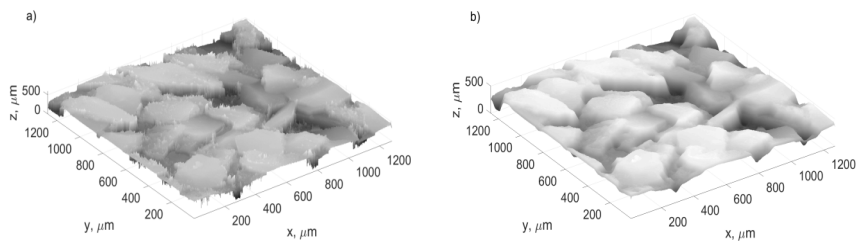

Fig. 1. Fragments of the abrasive tool active surface: a) before filtration; b) after filtration.

What is visible in the image registered using the confocal microscope is the measurement noise caused by short breaks in the signal, registered by the CCD detector. These breaks are a result of occurring steep abrasive grain slopes and deep indentations in the abrasive tool structure on the tool active surface. As a result, the non-existent sharp peaks or dales are visible in the image.

To filter the measured abrasive tool active surface, the average value of surface ordinates z_s in a slide window of size N was determined:

$$z_s(i,j) = \frac{1}{N^2 - 1} \sum_{n=i-N/2}^{N/2} \sum_{m=j-N/2}^{N/2} z(n,m) - z(i,j). \tag{2}$$

Next, the window central point ordinate z_c was modified in accordance with the following dependence:

$$z_c(i,j) = \begin{cases} z_c(i,j) & \text{for } |z_c(i,j) - z_s(i,j)| \leq \tau \\ z_s(i,j) & \text{for } |z_c(i,j) - z_s(i,j)| > \tau \end{cases}. \tag{3}$$

The data were filtered using a window of size $N = 5$ (6.25 μm) for $\tau = 0.1$ μm and a window of size $N = 20$ (25 μm) for $\tau = 25$ μm. An example of a filtered abrasive tool active surface fragment is presented in Fig. 1b. Filtering with a window of size $N = 5$ (6.25 μm) made it possible to smooth out the abrasive grain surface. Because the filtration window size is much smaller than the abrasive grain size, the borders between the abrasive grains were not blurred as a result of the filtration process. Filtering with a window of size $N = 20$ (25 μm) made it possible to remove the measurement noise, sharp peaks and dales on the abrasive tool surface. Smoothing out the abrasive grain surface and removing the measurement noise made it possible

to avoid, as a result of later abrasive grain detection, excessive abrasive tool active surface segmentation.

3. Methodology of abrasive grain detection using watershed segmentation

The watershed segmentation was used to detect abrasive grains on the abrasive tool active surface. The concept of watershed segmentation was derived from a method of determining watersheds in the field of hydrology. An important role in the watershed segmentation is played by the concept of a flood area [22, 26, 27]. In the case of a topographic surface, the beginning of the flood area is in the regional surface minima or the markers pointing to the image characteristic features.

In the recommended methodology, the topographic surface is understood to be a virtual copy of the abrasive grain active surface. The characteristic features of abrasive grain active surface are the abrasive grain tips which are selected to limit detection of numerous tips on a single abrasive grain surface. The operation of expanding flood areas was performed on the areas corresponding to the abrasive grain tips. "Dams" called watersheds were set in places where the flood areas would merge. The created watershed lines correspond to the borders between abrasive grains on the abrasive tool active surface.

A detailed diagram of the proposed methodology of detecting abrasive grains on the abrasive tool active surface is presented in Fig. 2.
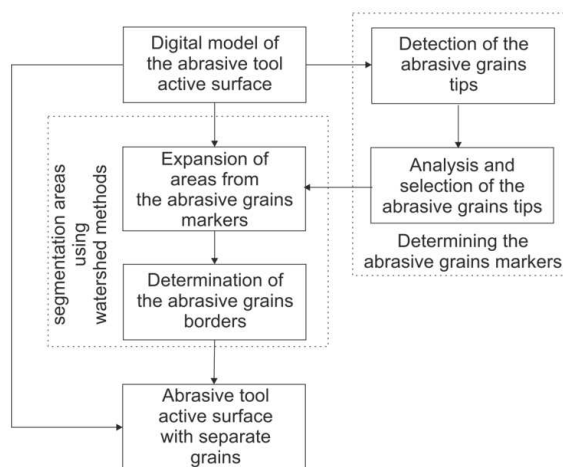
Fig. 2. Determining the abrasive grain borders.

The abrasive grains identified as a result of the watershed segmentation underwent further analysis. The parameters describing the abrasive grain shapes and their locations on the abrasive tool active surface were determined, and the parameters characterizing the volume of intergranular spaces were set.

3.1. Determining abrasive grain markers

The topographic surface contains many minima, and their number is additionally increased by noise, depending on the applied measurement method. Performing the watershed segmentation on such a surface results in identification of many areas that are irrelevant for detection of abrasive grains.

www.czasopisma.pan.pl   PAN   www.journals.pan.pl
POLSKA AKADEMIA NAUK

Metrol. Meas. Syst., Vol. 23 (2016), No. 4, pp. 567–577.

The number of local minima can be decreased using methods that simplify graphs describing relations between the characteristic surface points. Despite of the fact that the graphs characterize the surface, their simplification criterion regards only height parameters. The presented methodology limits the number of local minima using morphology analysis in order to detect the location of abrasive grain tips. The detected tips of abrasive grains determine the location of initial floodplains on the topographic surface.

To detect the abrasive grain tips, the topographic surface underwent the operation of opening by reconstruction, and then the areas of local minima were determined. A structural disc-shaped element B with a diameter S_B was used for the morphological operations. Application of the opening by reconstruction operation made it possible to skip all of the local minima in the image, whose areas were smaller than the size S_B of structural element.

The thus obtained density of a set of potential abrasive grains depends on the size of structural element used in the opening by reconstruction operation (Fig. 3a).
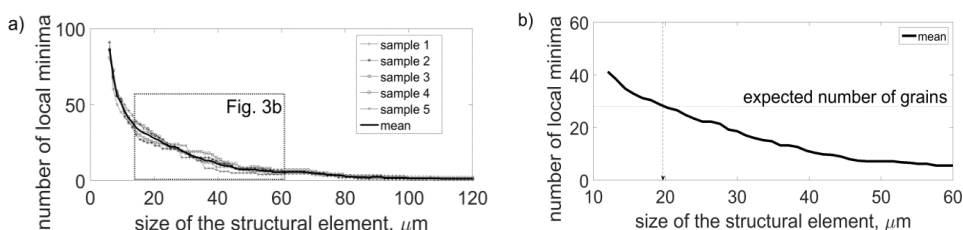

Fig. 3. The results of detecting the local minima: a) dependence between the size of structural element and the number of local minima, and b) selection of the structural element size.

To select the size S_B of structural element, visual evaluation of the abrasive tool active surface fragments is required to determine the average expected number of abrasive grains n_{gexp}. Abrasive grains visible on the measured specimens were counted manually and averaged (n_{gexp} = 28). On this basis, using the dependence presented in Fig. 3b, it was assumed that, after rounding up to the closest odd integer, the structural element size was $S_B = 19$ μm. For such parameters, a set W of potential abrasive grain tips on the abrasive tool surface was determined. The mappings of the set onto the topographic and the abrasive tool active surfaces are presented in Fig. 4.
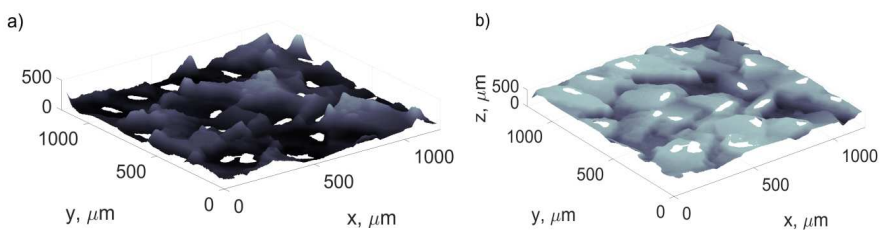

Fig. 4. The set W of potential abrasive grain tips mapped onto: a) the topographic surface G; b) the abrasive tool active surface Z.

Abrasive grains can be characterized by the presence of a few tips on their surface, especially in the case of abrasive machining operations, in which the dominant wear of abrasive grains is the effect of chipping their surface. To minimize the grain detection errors that occur when identifying a few tips within one abrasive grain, some areas were selected. A set W_D of tips

located at a distance smaller than the maximum abrasive grain size $d_{max} = 559$ μm was chosen for each of the potential abrasive grain tips.

Next, a few areas were connected, for which the maximum difference of the surface ordinates between the subsequent tips in set W_D was smaller than 5% of the maximum surface ordinate value ($\Delta h = 5\% \ St$).

3.2. Segmentation of abrasive grains using watershed method

The set W_D of tips, which constitute the regional minima of the topographic surface G, was assumed to be the beginning of the flood area. Next, by expansion of the areas, using the dilation operation, the "flooding" process was simulated:

$$G \oplus B = \{g + b : g \in G \wedge b \in B\}, \qquad (4)$$

where: $\oplus$ – Minkowski sum, and B – a structural element.

As a result of the segmentation, the flood areas were determined; after being mapped onto the tool active surface, the identified flood areas enabled to determine the abrasive grain borders (Fig. 5).
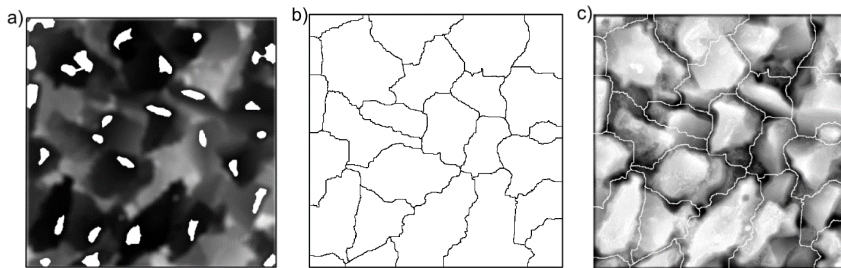

Fig. 5. The results of the abrasive tool detection process: a) the topographic surface with grain tip markers; b) the identified abrasive grain areas; c) the abrasive grain areas mapped onto the original surface.

Pre-filtering the measurement data and using the abrasive grain tips as markers of the local minima on the topographic surface results in obtaining a proper number of abrasive grain areas. Mapping the determined abrasive grain areas onto the abrasive tool active surface Z enables to determine the abrasive tool active surface topography parameters.

4. Evaluation of abrasive tool active surface

Selecting and indexing the abrasive grain areas on the abrasive tool active surface enabled to determine the geometric parameters of these areas and the statistical features that describe their location distribution. To obtain the abrasive tool active surface topography, the abrasive grain shapes, their locations on the abrasive tool active surface and the volume of intergranular spaces were evaluated.

4.1. Evaluation of abrasive grain shapes

Information on the abrasive grain shapes is crucial for evaluation and selection of parameters of shaping the abrasive grain active surface to obtain the required geometric parameter values that describe the machined surface. Evaluation of the parameters describing the abrasive grain shapes is also the basis for evaluation of the abrasive tool wear form.

A diagram illustrating the determined parameters of abrasive grain shape evaluation is presented in Fig. 6.
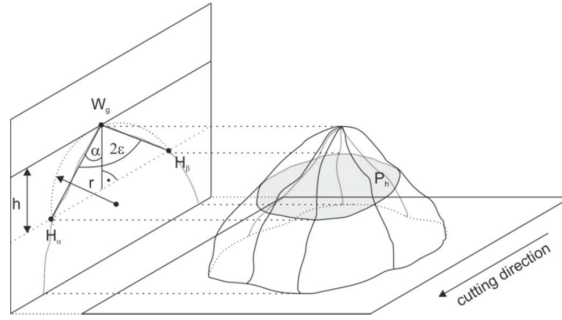
Fig. 6. A diagram illustrating the determined abrasive grain shape parameters.

For the measured abrasive tool active surface fragments, the following abrasive grain parameters were set. All of the parameters were determined for a given level h determined in relation to the grain tip W_g:

– The rake angles α and the abrasive grain tip angle 2ε.
– The radius r of the circle circumscribed on the abrasive grain tip – it is determined with the least squares method, passing the grain tip W_g and the points of crossing the side rake and the grain relief rake with the cut-off plane at a level h (points H_α and H_β).
– The coefficient F_g of space filling by grains – the coefficient value indicates a level V_z to which the space is filled by grains, which is the product of the grain section surface P_h and the cut-off level h.

Figure 7 presents a histogram of rake angles α and tip angles 2ε (for $h = 20$ µm). The value of angles α ranges from −87° to −32° (Fig. 7a). The negative value of rake angles of the abrasive grains (with the average value of −68°), typical for machining processes, is clearly seen.
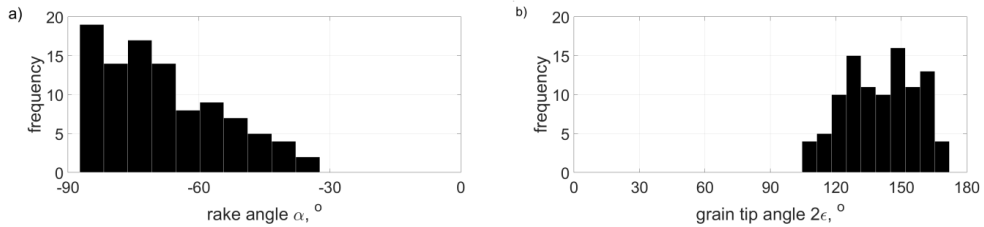

Fig. 7. A histogram of: a) rake angles α; b) tip angles 2ε on the abrasive grain active surface for $h = 20$ µm.
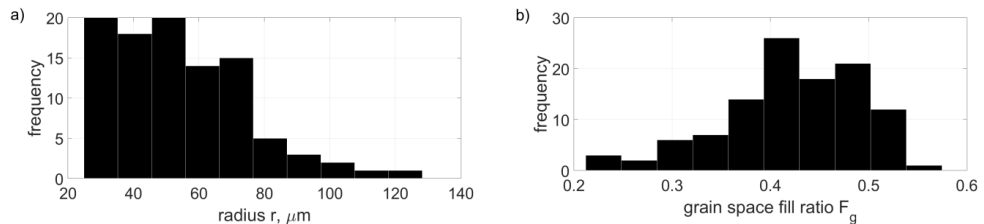

Fig. 8. A histogram of: a) radii r circumscribed on grain tips; b) the coefficient F_g of filling by grains the space on the abrasive tool active surface for $h = 20$ µm.

The range of grain tip angles from 120º to 160º includes 78% of all the abrasive grains (Fig. 7b). Different forms of distributions of radii *r* that circumscribe the abrasive grain tip (Fig. 8a) in relation to distributions of the grain tip angles *2ε* (Fig. 7b) are the result of the asymmetrical nature of location of the grain tip W_g in relation to the side rake H_α and side relief rake H_β points of crossing with the cut-off plane at the level *h*. This asymmetry is most probably the result of the process of dressing the abrasive tool active surface.

Figure 8b presents distribution of the grain space fill coefficient. The value of the coefficient ranges from 0.21 to 0.58 (with the average value of 0.42). The coefficient value indicates that a single abrasive grain has a medium capacity to remove approximately 42% of the volume of the machined material it has on it. Changing the value of the fill coefficient during machining, along with changing the abrasive grain tip angle value, as well as the value of the radius of the circle circumscribing the abrasive grain tip, may be the basis for evaluating the abrasive grain wear form.

4.2. Evaluation of abrasive grain location

Evaluation of the abrasive grain location is important in analyzing the grinding forces, the energy of grinding process and the size of cut layer cross-sections. The basic parameter of this analysis is the number of active grains per surface unit C_g and the average distance between grains l_{mean} on a given level *h* determined in relation to the maximum abrasive tool active surface ordinate. The average distance between the abrasive grain tips was set using Delaunay triangulation.
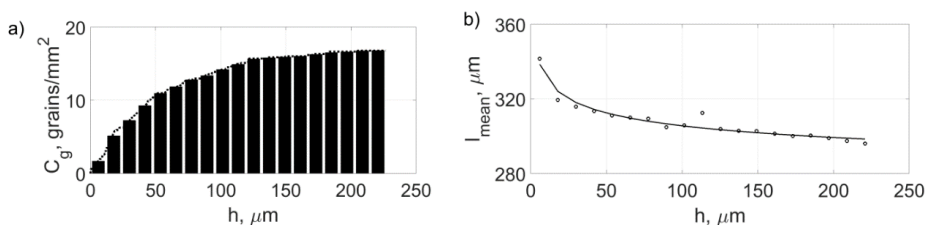
The results are presented in Fig. 9.

Fig. 9. Evaluation of the abrasive grain locations on the abrasive tool active surface in relation
to the cut-off level h: a) the average density of abrasive grains per unit area;
b) the average distance between abrasive grains.

Figure 9a presents a non-linear increase of the density of abrasive grains per unit area. Its value changes from 0.6 to 16 grains per mm^2. For a depth-of-cut value $h = 20$ μm, the average abrasive grain density is 6 grains/mm^2. The increase in the abrasive grain density for $h > 60$ μm is the result of lower locations of the abrasive grain layers . Due to a small size of the lower located abrasive grains in the microscopic image, the number of abrasive grain detection errors may increase, and a bond bridge isolation may occur.

The increase in the number of abrasive grains per surface unit results in a decrease in the average distance between abrasive grains (Fig. 9b). The average distance between the abrasive grains stabilizes on the level of $h = 200$ μm, at a value of approximately 300 μm.

4.3. Evaluation of intergranular spaces

An important form of abrasive grain wear is clogging of the active surface by removal products of the grinding process. Smearing the abrasive tool active surface makes it difficult to remove chips from the grinding zone, so the area of contact between the abrasive tool and

a workpiece increases. A greater area of contact causes increased friction and – therefore – increased temperature in the grinding zone, contributing to faster abrasive tool wear. This phenomenon becomes particularly important in the case of grinding soft non-alloy steels and nickel and chromium alloys (*e.g.* Inconel).

To evaluate the intergranular spaces on the abrasive tool active surface, the following quantities were determined: the average volume of intergranular spaces per unit area V_p and the average volume of intergranular spaces per grain V_g for a given cut-off level h. The analysis results are presented in Fig. 10.
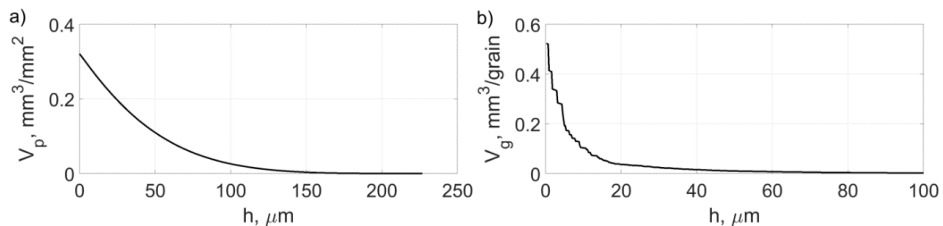

Fig. 10. The average volume of intergranular spaces on the abrasive tool active surface in relation to a cut-off level h per: a) surface unit V_p; b) grain V_g.

The maximum depth-of-cut value in machining processes usually does not exceed 30% of the average abrasive grain size d_{mean}. In the analyzed case ($d_{mean} = 356$ μm) − 100 μm below the highest ordinate value of the abrasive tool active surface – the volume of intergranular spaces enables to accumulate chips whose volume is approximately 0.025 mm^3/mm^2, which corresponds to the value of approximately 0.002 mm^3/grain. Because the analyzed abrasive grain is used in reciprocal internal cylindrical grinding operations, which results in a long path of cutting abrasive grains, lower depth-of-cut values are used. For a typical depth-of-cut value $h = 20$ μm, the average intergranular space volume per abrasive grain is approximately 0.037 mm^3/grain.

5. Conclusions

The presented analysis of the methodology of detection and evaluation of the abrasive tool active surface and the above presented analyses lead to the following conclusions:

– The use of an optical microscope with a dual confocal system enables to measure the surface of a grinding tool consisting of materials with different light reflection coefficients (abrasive grain material and bond material).

– Application of the watershed segmentation using abrasive grain tips as markers enables to identify abrasive grains on the abrasive tool active surface.

– Selecting and indexing abrasive grain areas on the abrasive tool active surface enables to determine the geometric parameters of these areas and the statistical features that describe their distribution. This information enables to evaluate the shape of abrasive grains and their locations on the abrasive tool active surface, as well as to assess the volume of intergranular spaces.

– Detection of grain tips using the local maxima method employing structural elements shaped as a 19 μm size disc (*i.e.*, 5% of the average abrasive grain size) enables to determine the expected number of abrasive grains.

– Aggregation of the neighboring abrasive grain tips for which the maximum difference of surface ordinates between them is less than 5% of the value of *St* parameters of the abrasive

tool active surface minimizes undesired detection of many tips on the surface of a single abrasive grain.

Using the above-presented methodology in evaluation of the abrasive tool active surface makes it possible to assess an influence of its shaping parameters on the abrasive grain geometric features, thereby enabling to assess their influence on the machined surface topography. The method also makes it possible to evaluate changes in the cutting capacity of abrasive tools during machining, which is particularly important in processes that select machining parameters to maximize the cutting capability.

Acknowledgments

Definitions

2ε – grain tip angle, deg
α – grain rake angle, deg
τ – filter threshold value, μm
a_d – dressing depth, mm
d_{max} – maximum abrasive grain size, μm
d_{mean} – mean abrasive grain size, μm
h – cut-off level, μm
l_{mean} – average distance between grains, μm
n_{exp} – expected number of grains
r – radius of the circle circumscribed on the abrasive tip, μm
x,y,z – coordinates, μm
v_d – peripheral speed of the dresser, m/s
v_{fd} – axial table feed speed during dressing cut, mm/rotation

B – structural element used in morphological operations
C_g – number of active grains per unit area, mm^{-2}
F_g – coefficient of space filling by a grain
G – topographic surface
N – size of slide window, points
P_h – grain section surface, μm^2
S_B – size of structural element, points
W – set of potential abrasive grain tips
W_d – set of potential abrasive grains tips located at a distance smaller than d
W_g – grain tip
V_p – average volume of intergranular spaces per unit area, mm^3/mm^2

References

[1] Kacalak, W., Tandecka, K. (2012). Effect of superfinishing methods kinematic features on the machined surface. *Journal of Machine Engineering*, 12(4), 35–48.

[2] Kacalak, W., Tandecka, K., (2012). Basics of forecasting superfinishing results be the diamond lapping films. *Journal of Machine Engineering*, 12(4), 49–62.

[3] Rowe, W.B. (2009). *Principles of modern grinding technology*. William Andrew, Elsevier.

[4] Marinescu, I.D., Hitchiner, M., Uhlmann, W., Rowe, W.B., Inasaki, I. (2007). *Handbook of machining with grinding wheels*. CRC Press, Taylor & Francis Group.

[5] Nadolny, K.(2015). Wear phenomena of grinding wheels with sol-gel alumina abrasive grains and glass-ceramic vitrified bond during internal cylindrical traverse grinding of 100Cr6 steel. *International Journal of Advance Manufacturing*, 77(1), 83–98.

[6] Lipiński, D., Kacalak, W. (2007. Assessment of the accuracy of the process of ceramics grinding with the use of fuzzy interference. *Adaptive and Natural Computing Algorithms, Lecture Notes in Computer Science*, 4431, 596–603.

[7] Blunt, L., Ebdon, S. (1996). The application of three-dimensional surface measurement techniques to characterizing grinding wheel topography. *International Journal of Machine Tools and Manufacture*, 36, 1207–1226.

[8] Matsuno, Y., Yamada, H., Harada, M., Kobayashi, A. (1975). Microtopography of the grinding wheel surface with SEM. *Annals of the CIRP*, 24, 237–242.

[9] Lachance, S., Warkentin, A., Bauer, R.J. (2003). Development of an automated system for measuring grinding wheel wear flats. *Journal of Manufacturing Systems*, 22, 130–135.

[10] Yan, L., Rong, Y.M., Feng, J., Zhi, X.Z. (2011). Three-dimension surface characterization of grinding wheel using white light interferometer. *International Journal of Advanced Manufacturing Technology*, 55, 133-141.

[11] Chen, X., Brian Rowe, W. (1996). Analysis and simulation of the grinding process. Part I: generation of the grinding wheel surface. *International Journal of Machine Tools and Manufacture*, 36, 871–882.

[12] Koshy, P., Ives, L.K., Jahanmir, S. (1999). Simulation of diamond-ground surfaces. *International Journal of Machine Tools and Manufacture*, 39, 1451–1470.

[13] Cooper, W.L. (2000). Grinding process size effect and kinematics numerical analysis. *Journal of Manufacturing Science and Engineering*, 122(1), 59–69.

[14] Zhou, X, Xi, F. (2002). Modeling and predicting surface roughness of the grinding process. *International Journal of Machine Tools and Manufacture*, 42, 969–977.

[15] Nguyen, T.A., Butler, D.L. (2005). Simulation of precision grinding process. Part I: generation of the grinding wheel surface. *International Journal of Machine Tools and Manufacture*, 45, 1321–1328.

[16] Xie, J., Xu, J., Tang, Y., Tamaki, J. (2008). 3D graphical evaluation of micron-scale protrusion topography of diamond grinding wheel. *International Journal of Machine Tools and Manufacture*, 48, 1254–1260.

[17] Xie, J., Tamaki, J. (2006). In-process evaluation of grit protrusion feature for fine diamond grinding wheel by means of electro-contact discharge dressing. *Journal of Materials Proc. Technology*, 180(1–3), 83–90.

[18] Nguyen, A.T., Butler, D.L. (2008). Correlation of grinding wheel topography and grinding performance: a study from a viewpoint of three-dimensional surface characterization. *Journal of Materials Proc. Technology*, 208, 14–23.

[19] Darafon, A. (2013). *Measuring and modelling of grinding wheel topography*. Ph.D. Thesis. Dalhousie University, Halifax.

[20] Bazan, A., Kawalec, A., Krok, M., Chmielik, I.P. (2014). The analysis of selected parameters of grains of CBN grinding wheels. *Mechanik*, 87(8–9), 49–57.

[21] Xie, J., Wei, F., Zheng, J.H., Tamaki, J., Kubo, A. (2011). 3D laser investigation on micron-scale grain protrusion topography of truncated diamond grinding wheel for precision grinding performance. *International Journal of Machine Tools and Manufacture*, 51, 411–419.

[22] Soille, P. (2004). *Morphological image analysis: principles and applications*. Springer-Verlag.

[23] Blunt, L., Jiang, X. (2003). *Advanced techniques for assessment surface topography*. Kogan Page Science.

[24] Lonardo, P.M., Trumpold, H., De Chiffre, L. (1996). Progress in 3D surface microtopography characterization. *Annals of the CIRP*, 45, 589–598.

[25] Lipiński, D., Kacalak, W., Tomkowski, R. (2014). Methodology of evaluation of abrasive tool wear with the use of laser scanning microscopy. *Scanning*, 36(1), 53-63, *http://dx.doi.org/10.1002/sca.21088*

[26] Beucher, S., Meyer, F. (1999). The morphological approach to segmentation: the watershed transformation. Dougherty, E.R (ed). *Mathematical morphology in image processing*. SPIE i IEEE Presses, Bellingham, WA, 433–481.

[27] Wu, Q., Merchant, F.A., Castleman, K.R. (2008). *Microscope image processing*. Elsevier.